

AD-A135 067

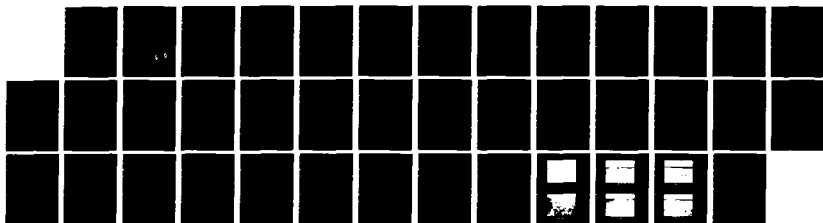
STUDY OF THE LUBRICATION MECHANISM OF THIN FILM
LUBRICATED CONCENTRATED S. (U) METAALINSTITUUT TNO
APELDOORN (NETHERLANDS) DEPT OF SURFACE T.

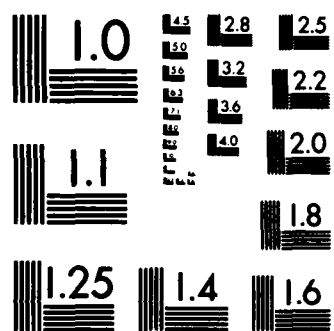
1/1

UNCLASSIFIED

A BEGELINGER ET AL. SEP 83 DAJA37-82-C-0465 F/G 11/8

NL





MICROCOPY RESOLUTION TEST CHART
NATIONAL BUREAU OF STANDARDS-1963-A

4

AD

AD-A135067

STUDY OF THE LUBRICATION MECHANISM OF THIN
FILM LUBRICATED CONCENTRATED STEEL CONTACTS

The influence of pre-treatment of the
steel on the load carrying capacity

Final Technical Report

by

A. Begelinger and A.W.J. de Gee

September 1983

EUROPEAN RESEARCH OFFICE

United States Army

London England

GRANT NUMBER DAJA 37-82-C-0465

DTIC
SELECTED
NOV 29 1983
S E D

Department of Surface Treatment and Tribology

Metaalinstuut TNO, P.O. Box 541, 7300 AM Apeldoorn, The Netherlands

Approved for Public Release; distribution unlimited

DTIC FILE COPY

20. Abstract (continuation)

→ transition from partial elastohydrodynamic lubrication to unlubricated contact ("scuffing regime"). When using liquid-nitrided surfaces, loading in excess of F_{Nc} leads to a transition from partial EHD lubrication to boundary lubrication. This shows that liquid-nitriding considerably increases the upper limit of the temperature range in which boundary lubrication is possible. ←

Depending on the composition of the steel substrate, the type of surface treatment and the running-in history, two instead of one F_{Nc} value may be found, i.e. F_{Nc1} and F_{Nc2} . At $F_N \geq F_{Nc1}$, immediate collapse of the EHD film occurs; at $F_{Nc2} < F_N < F_{Nc1}$ delayed collapse occurs, with delay times of the order of 1 hour; at $F_N < F_{Nc2}$ the EHD film survives six hours running, the lifetime of the crossed cylinder assembly probably being limited only by surface fatigue.

For untreated ball bearing steel 100Cr6, carburized surfaces and ion-nitrided surfaces, the values of F_{Nc1} range from 38 to 225 N, depending on the type of steel, the surface treatment and the running-in history; when using liquid nitrided surfaces, F_{Nc1} values range from 1000 to 1550 N, depending on the type of substrate material. For untreated ball bearing steel SAE 52100, carburized and ion-nitrided surfaces, the F_{Nc2} values range from 37.5 to 125 N, again depending on the type of steel, the surface treatment and the running-in history. For liquid-nitrided surfaces the F_{Nc2} values range from 850 to 1450 N.

1) U.S. designation: SAE 52100

Accession For	
NTIS GRA&I	<input checked="" type="checkbox"/>
DTIC TAB	<input type="checkbox"/>
Unannounced	<input type="checkbox"/>
Justification	
By	
Distribution/	
Availability Codes	
Dist	Avail and/or Special
A-1	



TABLE OF CONTENTS

	page
LIST OF ILLUSTRATIONS	2
LIST OF TABLES	3
LIST OF SYMBOLS	4
INTRODUCTION	5
DESCRIPTION OF SURFACES	5
EXPERIMENTAL	6
RESULTS	8
The transition process	8
The transition forces F_{Nc1} and F_{Nc2}	9
Wear rates in regime I in relation to the "white layer" on nitrided surfaces	10
DISCUSSION	11
SUGGESTIONS FOR FUTURE RESEARCH	11
REFERENCES	12
APPENDIX 1	13

LIST OF ILLUSTRATIONS

Fig. 1 Transition diagram for sliding concentrated steel contacts, operating fully submerged in a liquid lubricant of constant bulk temperature (schematic presentation).

f = coefficient of friction
k = specific wear rate (10^{-6} mm³/Nm).

Fig. 2 Coefficient of friction versus time for two tests, performed with liquid-nitrided surfaces of steel 34 Cr Al Mo 5 (F).

F_N = normal force
ΔV = volume wear, measured after termination of the tests.
No running-in (d* = 0 m).

Fig. 3 Coefficient of friction versus time for two tests, performed with liquid-nitrided surfaces of steel 42 Cr Mo 4 (E).

F_N = normal force
ΔV = volume wear, measured after termination of the tests.
No running-in (d* = 0 m).

Fig. 4 The relative difference $\frac{F_{Nc1} - F_{Nc2}}{F_{Nc2}}$. 100% for six different surfaces.

A - F : for explanation see Table 1
d* : running-in distance.

Fig. 5 Critical load value for immediate film collapse F_{Nc2} for six different surfaces.

A - F : for explanation see Table 1
d* : running-in distance.

Fig. 6 Critical load for delayed film collapse F_{Nc1} for six different surfaces.

A - F : for explanation see Table 1
d* : running-in distance.

Fig. 7-12 Structures of surfaces; see Appendix 1.

LIST OF TABLES

- Table 1 Survey of steels and surface treatments.
- Table 2 Results of F_{Nc} determinations for untreated ball bearing steel 100 Cr 6.
- Table 3 Results of F_{Nc} determinations for carburized steel 17 Cr Ni Mo 6.
- Table 4 Results of F_{Nc} determinations for ion-nitrided steel 42 Cr Mo 4.
- Table 5 Results of F_{Nc} determinations for ion-nitrided steel 34 Cr Al Mo 5.
- Table 6 Results of F_{Nc} determinations for liquid-nitrided steel 42 Cr Mo 4.
- Table 7 Results of F_{Nc} determinations for liquid-nitrided steel 34 Cr Al Mo 5.
- Table 8 Summary of friction coefficient results
- Table 9 F_{Nc1} and F_{Nc2} values from Tables 2 - 7.
- Table 10 Summary of wear results.
- Table 11 (Appendix 1) Chemical composition of steels
- Table 12 (Appendix 1) Surface treatments.

LIST OF SYMBOLS

d^*	: running-in distance	(m)
f	: coefficient of friction	(-)
F_N	: force	(N)
F_N^*	: running-in force	(N)
F_{Nc}	: load carrying capacity	(N)
F_{Nc1}	: load carrying capacity for immediate film collapse	(N)
F_{Nc2}	: load carrying capacity for delayed film collapse	(N)
F_{Nt}	: test force	(N)
r_1	: radius of curvature of stationary cylindrical specimen	(mm)
r_2	: radius of curvature of rotating ring	(mm)
R	: electrical contact resistance	
R_a	: center-line-average (c.l.a.) roughness value	(μm)
t	: time	(s or min)
t_d	: delay time	(min)
v	: speed	(m/s)
v^*	: running-in speed	(m/s)
v_t	: test speed	(m/s)
ΔV	: volume wear	(mm^3)
η	: dynamic viscosity	(Pa.s)

INTRODUCTION

According to our research proposal of 16 July 1980, the effect of the surface treatments carburizing, ion-nitriding and liquid-nitriding (nitrocarburizing) on the load carrying capacity of thin film lubricated concentrated steel contacts was to be studied, the effect of running-in to be taken into account. The surface treatments were to be performed by third parties, to be selected by TNO.

It was agreed to perform the following tests:

The load carrying capacity F_{Nc} of thin film lubricated surfaces (either virginal or run-in) was to be determined by performing separate two-minutes tests with crossed cylinder specimens (c.f. ref. 1), at different values of test force F_{Nc} , recording friction and wear as parameters, characteristic for the regime of lubrication. The test speed v_t was to be 4 m/s. At this speed untreated surfaces of ball bearing steel 100Cr6 (SAE 52100) run to the right of the bifurcation point S (transition from regime I to regime III; see Fig. 1).

Running-in was to be performed at a running-in speed v^* of 0.1 m/s, at running-in distances d^* of 30 m and 300 m, respectively.

All tests were to be performed in marine diesel engine oil of 60°C, having a dynamic viscosity of $\eta = 6 \cdot 10^{-2}$ Pa.s.

DESCRIPTION OF SURFACES

A survey of steels and surface treatments, studied in the present research programme, is given in Table 1.

A detailed description with micro-photographs is given in Appendix 1. Table 1 shows that, when applying ion-nitriding or liquid-nitriding, two different substrate materials were used, i.e. steel 42CrMo4 and steel 34CrAlMo5. The aluminium containing steel is a typical "nitriding steel", in which the aluminium promotes the diffusion of nitrogen into the material. Usually such aluminium containing material is applied only in the case of gas-nitriding or ion-nitriding. In the case of liquid-nitriding addition of aluminium to the substrate is considered to be superfluous in most practical

cases. Still, also in the case of liquid-nitriding the presence of aluminium may promote the formation of a surface layer of better quality.

In the present test programme identical surfaces were combined, i.e. 100 Cr 6 / 100 Cr 6, carburized, 17 Cr Ni Mo 6 / carburized 17 Cr Ni Mo 6, etc.

EXPERIMENTAL

In the first quarter of the present contract period tests were run with untreated specimens of ball bearing steel 100 Cr 6 (SAE 52100) at $F_N^* = 0$ (no running-in) and at $F_N^* = 450$ N and $d^* = 30$ m. The results of these tests have been reported in our progress report of 12 November 1982.

It was shown that - without running-in - the usual sharp transition occurred; the load carrying capacity F_{Nc} was found to fall between 50 N and 60 N, which tallied with previous observations.

With running-in ($F_N^* = 450$ N), a delay time (called "dwell-time" in the progress report) is observed, again in accordance with earlier work (ref. 1). However, while in the past ('79-'80) it was assumed that if an EHD film survives a two-minute test, it will survive infinitely (i.e. provided that surface fatigue does not occur), the results found in the first quarter showed this assumption to be false. Given enough time (up to 1 hour) a transition from the EHD regime to the scuffing regime occurred, even under a normal force of 75 N.

In fact the results permitted the definition of two separate F_{Nc} values, i.e. one (F_{Nc1}), at the application of which immediate collapse of the EHD film occurs and another (F_{Nc2}), at the application of which delayed collapse occurs. Without running-in F_{Nc1} and F_{Nc2} co-incide.

From a technical (application-oriented) point of view, both F_{Nc1} and F_{Nc2} can be important. A high F_{Nc1} value enables the system to survive a brief period of overloading (good "emergency properties"), while on the other hand a high F_{Nc2} value permits prolonged running under relatively high normal loads.

Obviously the above results had important consequences for the performing of the remaining test programme. In fact it was agreed between TNO and the Army European Research Office in London to proceed with determining the relation between normal test force F_{Nt} and delay time t_d for all the surfaces to be

tested and for both running-in distances (30 m and 300 m).

This resulted in the following experimental procedure:

As in previous work (see ref. 1) the tests were carried out with the TNO Tribometer in marine diesel engine oil of 60°C. In order to obtain the crossed cylinder geometry, stationary cylindrical specimens with radii of curvature $r_1 = 6$ mm were mated with rotating cylinders (ring) with radii $r_2 = 73$ mm. Stationary as well as rotating specimens were made from ball bearing steel 100Cr6 (SAE 52100). The contact geometry thus obtained approached the geometry of cams and tappets quite well.

The stationary specimens were obtained by machining cylindrical surfaces with $r_1 = 6$ mm at the outer ends of cylindrical pins with 8 mm diameter. As the rings could be moved axially, relative to the stationary specimens, three to five individual tests could be performed on one ring surface.

In all tests the surface roughness of pins and rings amounted to $R_a = 0.15 - 0.17$ μm c.l.a.

Running-in was performed at $v^* = 0.1$ m/s; the running-in distance being 30 m (300 s; 126 revolutions of the ring) or 300 m (3000 s; 1260 revolutions of the ring). The running-in force F_N^* was 300 N for all specimen combinations (in the preliminary tests, the results of which are reported in the first progress report of this contract period, F_N^* was 450 N). Under these conditions of load and speed, the system ran under conditions of partial EHD (regime I in Fig. 1), which was verified by measuring friction (coefficient of friction of the order of 0.05) and electrical contact resistance ($R > 10^6 \Omega$).

The load carrying capacity F_{Nc} at $v = v_t$ of virginal as well as run-in surfaces was determined by performing separate tests at different values of normal force, recording friction and wear as parameters, characteristic for the regime of lubrication.

After applying the normal test force in less than 0.2 s, each individual test was continued until a clearly marked transition had occurred or until $t = 360$ min.

In cases where a transition occurred, each test was continued for a period of time Δt after transition, i.e.

$$t = t_d + \Delta t$$

In the case of untreated ball bearing steel, carburized steels and ion-nitrided steels Δt amounted to 6 seconds, in the case of liquid-nitrided steels Δt varied from 1 - 20 min.

RESULTS

The numerical results of the experiments are presented in Tables 2-7. The results are analysed in detail in the following paragraphs.

The transition process

The type of transition which occurs at $F_{N_t} > F_{N_{c2}}$, is characterized primarily by the coefficient of friction, measured immediately upon loading (f_1) and at the end of the test (f_2), respectively. Tables 2-7 show that, for each combination of surface and running-in distance an $F_{N_{c2}}$ value can be defined, below which friction remains at the level of 0.03-0.06 during the entire test, i.e. during 360 minutes. Clearly at $F_{N_t} < F_{N_{c2}}$ the system runs in regime I of Fig. 1.

At $F_{N_t} > F_{N_{c2}}$ immediate or delayed transfer to another lubrication regime occurs, delay times ranging from 1 - 81 min, depending on the type of surface, the running-in history and the value of F_{N_t} . Tables 2-7 show that the transition, which occurs ultimately, leads to f_2 values in the range of 0.31 - 0.51 in case of surfaces A, B, C or D and to f_2 values in the range of 0.17 - 0.24 in the case of surfaces E and F. This is shown in a condensed form in Table 8, in which the friction results, presented in Tables 2-7, are summarized.

On the strength of these friction results alone, it would be justified to conclude that, in the case of surfaces A, B, C and D, a transition from regime I to regime III occurs, while, in the case of surfaces E and F, the transition is from regime I to regime II. Additional and conclusive evidence that this is indeed the case, is derived from wear measurements, after termination of the tests. Tables 2-7 show that, for surfaces A, B, C and D, transition leads to an increase in wear rate $\Delta V / F_{N_t} \cdot v \cdot t$ by some four decades, while, for materials E and F, this increase in wear rate is of the order of 1 - 2 decade(s) only.

A closer analysis of the friction-time recordings, obtained when testing surfaces A, B, C and D shows that in these cases friction in regime I is low and constant. This is also true for surfaces of type F. This is shown in Fig. 2, which depicts the coefficient of friction f versus time t behaviour for tests, performed with material F under normal forces F_N of, respectively, 1400 N and 1500 N at $d^* = 0$.

Fig. 3 shows that surfaces of type E behave somewhat differently, in that, also at normal force values $F_{Nt} < F_{Nc2}$, the $f-t$ tracing is somewhat irregular. In this case, however, the highest friction peaks never exceed $f = 0.07$, which means that the system remains running in regime I. The latter also follows from the volume wear, measured after termination of the tests, which amounts to 0.06 mm^3 at $F_{Nt} > F_{Nc2}$ and to 2.1 mm^3 at $F_{Nt} < F_{Nc2}$.

Obviously the above results are very favourable for the liquid nitrided surfaces, in particular for surfaces of type F (Al-containing steel).

The transition forces F_{Nc1} and F_{Nc2}

The best estimates of the transition forces F_{Nc1} and F_{Nc2} are given in Tables 2-7 and are summarized in Table 9.

Firstly it can be seen that for surfaces of type A and B, which are not run-in ($d^* = 0$), $F_{Nc1} = F_{Nc2}$; thus in these cases delayed transition does not occur. In all other cases delayed transition does occur. The contribution of such delayed transition to temporary load carrying capacity varies considerably from one case to the other. This is shown in the last column of Table 9, in which the values of the ratio $\frac{F_{Nc1} - F_{Nc2}}{F_{Nc2}}$, expressed as a percentage, are given. The same information is presented in a graphical form in Fig. 4. It can be seen that delayed transition contributes to load carrying capacity in a substantial way only in the case of run-in surfaces of types A and B and run-in *and* virginal surfaces of type C. Further it should be noted that, in the case of surfaces of types B and C, running-in for longer periods of time ($d^* = 300 \text{ m}$) is *not* particularly favourable.

The F_{Nc1} and F_{Nc2} values are shown graphically in Figs. 5 and 6, respectively. It can be seen that - on the average - carburizing (B) and ion-nitriding (C, D) do not contribute much to load carrying capacity, when compared to the

behaviour of untreated ball bearing steel (A). On the other hand liquid-nitriding (E, F) is found to be extremely beneficial, in particular if a typical "nitriding steel", containing Al (F), is used as a substrate material. Clearly, the latter also holds for the ion-nitrided surfaces, were surfaces D behave better than surfaces C.

Running-in is found to improve the load carrying capacities F_{NC1} and F_{NC2} of surfaces A and B considerably. However, with the exception of the F_{NC1} values of surfaces of type C, running-in does not affect the load carrying capacities of ion- or liquid-nitrided surfaces.

As far as the F_{NC2} values are concerned, a tenfold increase in running-in distance (i.e. $d^* = 300$ m instead of $d^* = 30$ m) has no effect at all; in the case of the F_{NC1} values, longer running-in is detrimental rather than beneficial in two out of three cases (i.e. for surfaces of type B and C).

Wear rates in regime I in relation to the "white layer" on nitrided surfaces

The wear results, obtained after running in regime I are summarized in Table 10. It can be seen that the wear rates $\Delta V / F_{Nt} \cdot v \cdot t$ are very small in all cases; still there are quite pronounced differences from one type of surface to the other. In fact, as far as this criterion is concerned, the surfaces clearly rank in order of decreasing quality as follows:

D
A
B, C, E
F

Clearly this ranking correlates neither with the transition behaviour (in which surfaces of type E and F excel), nor with the Vickers Hardness values of the surface. The latter can be explained by assuming that in regime I the wear mechanism is that of corrosive wear, in which material is removed from the surfaces in the form of oxides or other chemical reaction products.

A wear rate of approx. $0.0085 \cdot 10^{-6} \text{ mm}^3/\text{Nm}$, measured after 6 hours of running (surfaces of type F) corresponds to a wear depth of the stationary specimen of approx. $150 \mu\text{m}$. As the white layer on the liquid-nitrided pins is from 6 to $10 \mu\text{m}$ thick, the white layer on the stationary specimen must have been worn through within 20 min. On the other hand, a similar wear of the ring would cause a wear scar with a depth of only a few micrometers. Thus, it were to be expected that the white layer on the stationary surfaces should be completely worn through, while that on the ring surfaces would still be visible. Metallographic examination of worn surfaces of type F showed this to be the case.

As the first breakthrough of the white layer on the stationary specimens of surfaces F must have occurred quite early in the process (i.e. within some 20 min), it can be concluded that breakthrough of the white layer on the stationary specimen does not influence the friction behaviour in any measurable way.

DISCUSSION

The results show quite clearly the superiority of the liquid-nitriding process for the prevention of scuffing under conditions of high-speed sliding contact. This is in line with recent results, obtained in the European motorcar industry (ref. 2). The disappointing results, obtained with ion-nitriding, correlate excellently with recent research performed by T.U. Aachen and Kloekner Ionon Industry (ref. 3).

It is somewhat surprising that the beneficial effect of aluminium in the substrate material manifests itself quite significantly, not only in the case of ion-nitrided surfaces but also in the case of liquid nitrided surfaces. In fact it is generally assumed that the use of typical "nitriding steels" does not contribute significantly to the quality of liquid-nitrided surfaces. The present results indicate that the use of such steels may significantly increase the load carrying capacity.

A possible explanation for the superiority of liquid-nitrided surfaces over ion-nitrided surfaces as far as scuffing prevention is concerned, is that liquid-nitrided surfaces possess micro-porosity, the pores at the surface acting as oil supply pockets (c.f. ref. 4). This hypothesis might be tested by studying surfaces with different degrees of porosity, for instance obtained by subjecting porous surfaces to hot isostatic pressing (HIP) at different pressure levels.

SUGGESTIONS FOR FUTURE RESEARCH

Possible future research objects might be aimed at the following objectives:

1. study of the effect of surface porosity as proposed above
2. study of other surface treatments, among others *gas nitriding*
3. determination of the load carrying capacities of non-identical surfaces and the effect of the geometry thereupon (e.g. liquid-nitrided pins on

carburized rings; carburized pins on liquid-nitrided rings)

4. performance of tests at a lower test speed v_t , for instance $v_t = 0.5$ m/s.

REFERENCES

- 1) A. Begelinger and A.W.J. de Gee, "Failure of thin-film lubrication - the effect of running-in on the load carrying capacity of thin-film lubricated concentrated contacts", Transactions ASME - JOLT, 103/2, 1981, 203-208.
- 2) Anon., "First U.K. Sursulf plant installed for diesel engine crankshafts", Metallurgia, Dec. 1982, 644-645.
- 3) Tribology (in German), Conference Volume, the 2nd presentation of R & D programmes sponsored by the Federal Ministry of Research and Technology (abbr. in German: BMFT), 1983, issued by DFVLR, Springer Verlag, Berlin, New York, Tokyo.
- 4) G. Salomon, "Tribology in German, Part 2: Surface treatment and wear analysis", Lub. Eng. 37, 11, (1981), 634-636.

DESCRIPTION OF STEELS AND SURFACE TREATMENTS

The chemical composition of the steels is given in Table 11. It should be noted that steel 34CrAlMo5 is a typical "nitriding steel" in which the aluminium promotes the diffusion of nitrogen into the material.

Particulars on the surface treatments are given in Table 12.

Carburizing was performed in an atmosphere of hydrocarbon gas (mixture of methane and propane). After treatment at 900°C, i.e. above the ferrite/austenite transformation temperature, the specimens were quenched to develop an essentially martensitic structure and finally tempered at 170°C. Prior to using the specimens, the surfaces were ground to the desired surface roughness (i.e. $R_a = 0.15 - 0.17 \mu\text{m c.l.a.}$).

The resulting structure is shown in Fig. 7 at 50 x magnification and in Fig. 8 at 500 x magnification. Fig. 7 shows that the carburized layer penetrates to a depth of about 1 mm into the material. The hardness, measured at the surface, is 720 Vickers.

Ion-nitriding was performed in an atmosphere of dissociated ammonia. Under the action of an applied voltage, the gases ionized and bombarded the negatively charged specimen, thereby heating it up to the processing temperature of 540°C and allowing nitrogen to diffuse into the surface. After treatment the specimens were slowly cooled to room temperature.

Figs. 9 and 10 show micrographs of, respectively, ion-nitrided steels 42CrMo4 and 34CrAlMo5. It can be seen that in both cases a white layer is formed, whereby - due the presence of aluminium - the transition from white layer to nitrided inner structure is much more gradual in steel 34CrAlMo5 than in steel 42CrMo4. The hardness values, measured at the surface, are, respectively, 650 Vickers (42CrMo4) and 1020 Vickers (34CrAlMo5).

The liquid nitriding (also called liquid nitrocarburizing) process was performed according to the proprietary Tenifer process. In this process active alkali metal cyanates are formed out of a mixture of sodium and potassium cyanides, carbonates and chlorides, whereby cyanate formation is stimulated by the injection of dry air. As in the case of ion-nitriding, a white compound layer of

ϵ carbonitride forms on top of a diffusion layer. The results in the form of micrographs are shown in Figs. 11 and 12 for steels 42CrMo4 and 34CrAlMo5, respectively. Again the transition from white layer to diffusion layer is more gradual in the case of the aluminium containing substrate material. Hardness values, measured at the surface, are, respectively, 560 and 970 Vickers.

Table 1

Survey of steels and surface treatments

Symbol	German standard number	Surface treatment	Code
100 Cr 6	1.3505	none	A
17 Cr Ni Mo 6	1.6587	carburizing	B
42 Cr Mo 4	1.7225	ion-nitriding	C
34 Cr Al Mo 5	1.8507	"-	D
42 Cr Mo 4	1.7225	liquid nitriding	E
34 Cr Al Mo 5	1.8507	"-	F

See Appendix 1 for a detailed description of steels and surface treatments.

Table 2

Results of F_{Nc} determinations for untreated ball bearing steel 100Cr 6 (A)

Running-in speed v^* : 0.1 m/s
 Test speed v_t : 4 m/s
 Lubricant : Marine diesel engine oil of 60°C
 R_a value contacting surfaces : 0.15 - 0.17 μm c.l.a.
 Test duration $t = t_d + 0.1$ min, with a maximum value of 360 min.

F_N^* (N)	F_{Nt} (N)	t_d (min)	f_1	f_2	$\frac{\Delta V}{F_{Nt} \cdot v \cdot t}$ $10^{-6} \frac{\text{mm}^3}{\text{Nm}}$	F_{Nc1} (N)	F_{Nc2} (N)
0	40	> 360	0.04	0.04	0.003	55	55
	50	> 360	0.04	0.04	0.004		
	60	0	0.46	-	>10		
	80	0	0.48	-	>10		
30	50	> 360	0.03	0.03	0.003	300	87.5
	75	> 360	0.03	0.03	0.004		
	100	49	0.03	0.43	>10		
	150	47	0.03	0.45	>10		
	200	32	0.03	0.46	>10		
	250	2	0.03	0.48	>10		
	300	1	0.03	0.48	>10		
350	0	0.48	-	>10			
300	50	> 360	0.03	0.03	0.002	300	87.5
	75	> 360	0.03	0.03	0.004		
	100	39	0.03	0.45	>10		
	150	3	0.03	0.46	>10		
	200	2	0.03	0.46	>10		
	250	1	0.03	0.46	>10		
	300	0	0.47	-	>10		

- F_N^* : running-in force
- F_{Nt} : test force
- t : test duration
- t_d : delay time
- f_1 : coefficient of friction, measured immediately upon loading
- f_2 : coefficient of friction, measured at the end of the test
- ΔV : volume wear, measured after termination of the test
- F_{Nc1} : normal force at which immediate film collapse occurs (approximate value)
- F_{Nc2} : normal force at which delayed film collapse occurs (approximate value)

Table 3

Results of F_{Nc} determinations for carburized steel 17CrNiMo 6 (B)
 (see Table 2 for test conditions and explanation of symbols)

F_N^* (N)	F_{Nt} (N)	t_d (min)	f_1	f_2	$\frac{\Delta V}{F_{Nt} \cdot v \cdot t}$ $10^{-6} \frac{\text{mm}^3}{\text{Nm}}$	F_{Nc1} (N)	F_{Nc2} (N)
0	25	>360	0.03	0.03	0.004	37.5	37.5
	50	0	0.40	-	>10		
	60	0	0.41	-	>10		
30	50	>360	0.03	0.03	0.008	275	62.5
	75	45	0.03	0.51	>10		
	100	40	0.03	0.48	>10		
	150	30	0.03	0.49	>10		
	200	4	0.03	0.50	>10		
	250	2	0.03	0.51	>10		
	300	0	0.48	-	>10		
300	50	>360	0.03	0.03	0.007	175	62.5
	75	53	0.03	0.49	>10		
	100	2	0.03	0.50	>10		
	150	1	0.03	0.51	>10		
	200	0	0.49	-	>10		

Table 4

Results of F_{Nc} determinations for ion-nitrided steel 42CrMo4 (C)
 (see Table 2 for test conditions and explanation of symbols)

F_N^* (N)	F_{Nt} (N)	t_d (min)	f_1	f_2	$\frac{\Delta V}{F_{Nt} \cdot v \cdot t}$ $10^{-6} \frac{\text{mm}^3}{\text{Nm}}$	F_{Nc1} (N)	F_{Nc2} (N)
0	25	>360	0.05	0.05	0.005	87.5	37.5
	50	42	0.05	0.38	>10		
	75	36	0.05	0.38	>10		
	100	0	0.48	-	>10		
	150	0	0.48	-	>10		
30	25	>360	0.05	0.05	0.006	175	37.5
	50	40	0.05	0.30	>10		
	75	34	0.05	0.31	>10		
	100	4	0.05	0.38	>10		
	150	1	0.05	0.40	>10		
	200	0	0.39	-	>10		
300	25	>360	0.05	0.05	0.005	87.5	37.5
	50	39	0.05	0.32	>10		
	75	2	0.05	0.38	>10		
	100	0	0.39	-	>10		

Table 5

Results of F_{Nc} determinations for ion-nitrided steel 34CrAlMo 5 (D)

(see Table 2 for test conditions and explanation of symbols)

F_N^* (N)	F_{Nt} (N)	t_d (min)	f_1	f_2	$\frac{\Delta V}{F_{Nt} \cdot v \cdot t}$ $10^{-6} \frac{\text{mm}^3}{\text{Nm}}$	F_{Nc1} (N)	F_{Nc2} (N)
0	75	>360	0.05	0.05	0.001	175	125
	100	>360	0.05	0.05	0.002		
	150	81	0.05	0.35	>10		
	200	0	0.42	-	>10		
	250	0	0.45	-	>10		
30	75	>360	0.06	0.06	0.002	175	125
	100	>360	0.05	0.05	0.002		
	150	3	0.05	0.46	>10		
	200	0	0.44	-	>10		
300	75	>360	0.06	0.06	0.002	175	125
	100	>360	0.06	0.06	0.002		
	150	1	0.06	0.46	>10		
	200	0	0.46	-	>10		

Table 6

Results of F_{Nc} determinations for liquid-nitrided steel 42 Cr Mo 4 (E)

(see Table 2 for test conditions)

t = test duration: see Table 2 for further explanation of symbols

F_N^* (N)	F_{Nt} (N)	t (min)	t_d (min)	f_1	f_2	$\frac{\Delta V}{F_{Nt} \cdot v \cdot t}$ $10^{-6} \frac{\text{mm}^3}{\text{Nm}}$	F_{Nc1} (N)	F_{Nc2} (N)
0	600	>360	>360	0.05	0.03	0.004	1150	850
	700	>360	>360	0.05	0.04	0.004		
	800	>360	>360	0.05	0.04	0.005		
	900	60	50	0.05	0.17	0.5		
	1000	5	4	0.06	0.22	0.6		
	1100	2	1	0.06	0.24	0.8		
	1200	0	0	0.24	-	1.1		
30	700	>360	>360	0.05	0.04	0.004	1150	850
	800	>360	>360	0.05	0.04	0.004		
	900	40	30	0.05	0.22	0.5		
	1000	10	8	0.05	0.22	0.5		
	1100	1	1	0.05	0.24	0.7		
	1200	0	0	0.24	-	0.8		
300	700	>360	>360	0.05	0.04	0.004	1150	850
	800	>360	>360	0.05	0.04	0.004		
	900	60	40	0.05	0.23	0.6		
	1000	16	8	0.05	0.24	0.8		
	1100	2	1	0.05	0.24	1.1		
	1200	0	0	0.24	-	1.1		

Table 7

Results of F_{Nc} determinations for liquid-nitrided steel 34CrAlMo 5 (F)

(see Table 2 for test conditions)

t = test duration; see Table 2 for further explanation of symbols

F_N^* (N)	F_{Nt} (N)	t (min)	t_d (min)	f_1	f_2	$\frac{\Delta V}{F_{Nt} \cdot v \cdot t}$ $10^{-6} \frac{\text{mm}^3}{\text{Nm}}$	F_{Nc1} (N)	F_{Nc2} (N)
0	1200	>360	>360	0.06	0.04	0.008	1650	1450
	1300	>360	>360	0.06	0.20	0.008		
	1400	>360	>360	0.06	0.20	0.009		
	1500	23	20	0.06	0.22	0.2		
	1600	2	1	0.06	0.22	0.4		
	1700	0	0	0.23	-	0.5		
30	1200	>360	>360	0.06	0.04	0.009	1650	1450
	1300	>360	>360	0.06	0.04	0.009		
	1400	>360	>360	0.06	0.04	0.009		
	1500	37	20	0.05	0.18	0.2		
	1600	2	1	0.05	0.20	0.3		
	1700	0	0	0.22	-	0.3		
300	1200	>360	>360	0.06	0.04	0.08	1650	1450
	1300	>360	>360	0.06	0.04	0.09		
	1400	>360	>360	0.06	0.04	0.09		
	1500	50	45	0.05	0.18	0.3		
	1600	3	2	0.05	0.21	0.4		
	1700	0	0	0.22	-	0.5		

Table 8

Summary of friction coefficient results

Material code	f_1	f_2	transition ^{*)}
A	0.03 - 0.04	0.46 - 0.48	I → III
B	0.03	0.40 - 0.51	I → III
C	0.05	0.31 - 0.48	I → III
D	0.05 - 0.06	0.42 - 0.46	I → III
E	0.03 - 0.06	0.17 - 0.24	I → II
F	0.04 - 0.06	0.18 - 0.23	I → II

^{*)} c.f. Fig. 1

Table 9

F_{Nc1} and F_{Nc2} values from Tables 2-7 (approximate values)

Material code	Running-in distance d* (m)	F_{Nc1}	F_{Nc2}	$\frac{F_{Nc1} - F_{Nc2}}{F_{Nc2}}$ (%)
A	-	55	55	0
	30	300	87.5	243
	300	300	87.5	243
B	-	37.5	37.5	0
	30	275	62.5	340
	300	175	62.5	180
C	-	87.5	37.5	133
	30	175	37.5	367
	300	87.5	37.5	133
D	-	175	125	40
	30	175	125	40
	300	175	125	40
E	-	1150	850	35
	30	1150	850	35
	300	1150	850	35
F	-	1650	1450	14
	30	1650	1450	14
	300	1650	1450	14

Table 10

Summary of wear results (regime I)

Material code	$\Delta V / F_{N_t} \cdot v \cdot t$ ($10^{-6} \text{ mm}^3/\text{Nm}$)	Vickers Hardness
A	0.002 - 0.004	800
B	0.004 - 0.008	720
C	0.005 - 0.006	560
D	0.001 - 0.002	970
E	0.004 - 0.005	650
F	0.008 - 0.009	1020

Table 11

Chemical composition of steels (wt.%)

Symbol	German standard number	C	Si	Mn	Cr	Ni	Mo	Al
100 Cr 6	1.3505	1.00	0.17	0.32	1.52	0.10	-	-
17 Cr Ni Mo 6	1.6587	0.16	0.18	0.50	1.63	1.50	0.27	-
42 Cr Mo 4	1.7225	0.41	0.22	0.72	1.10	0.38	0.20	-
34 Cr Al Mo 5	1.8507	0.36	0.23	0.68	1.22	-	0.22	1.00

Table 12

Surface treatments

Surface treatment	treatment temperature (°C)	treatment duration (h)
carburizing	900	3
ion-nitriding	540	30
liquid-nitriding	570	2

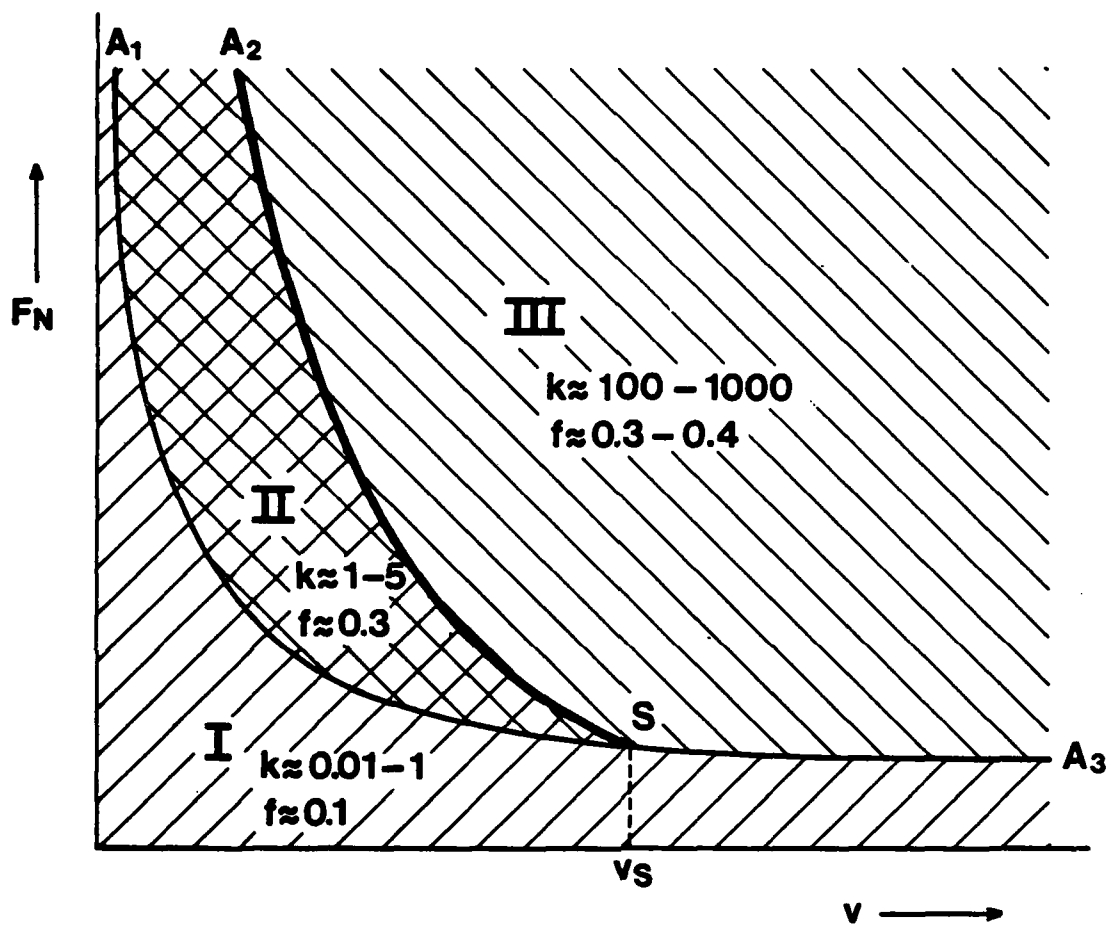


Fig. 1 Transition diagram for sliding concentrated steel contacts, operating fully submerged in a liquid lubricant of constant bulk temperature (schematic presentation).

f = coefficient of friction
 k = specific wear rate (10^{-6} mm³/Nm).

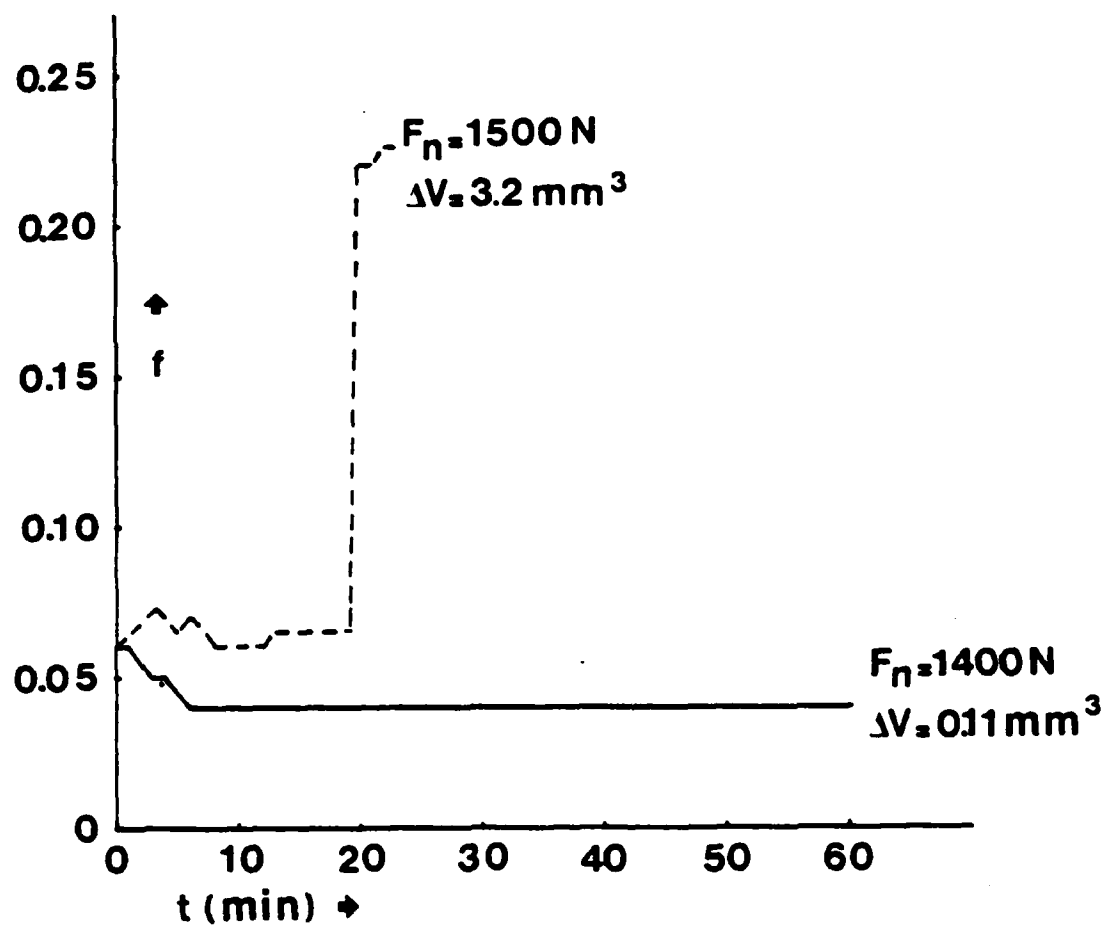


Fig. 2 Coefficient of friction versus time for two tests, performed with liquid-nitrided surfaces of steel 34CrAlMo 5 (F).

F_N = normal force

ΔV = volume wear, measured after termination of the tests.

No running-in ($d^* = 0 \text{ m}$).

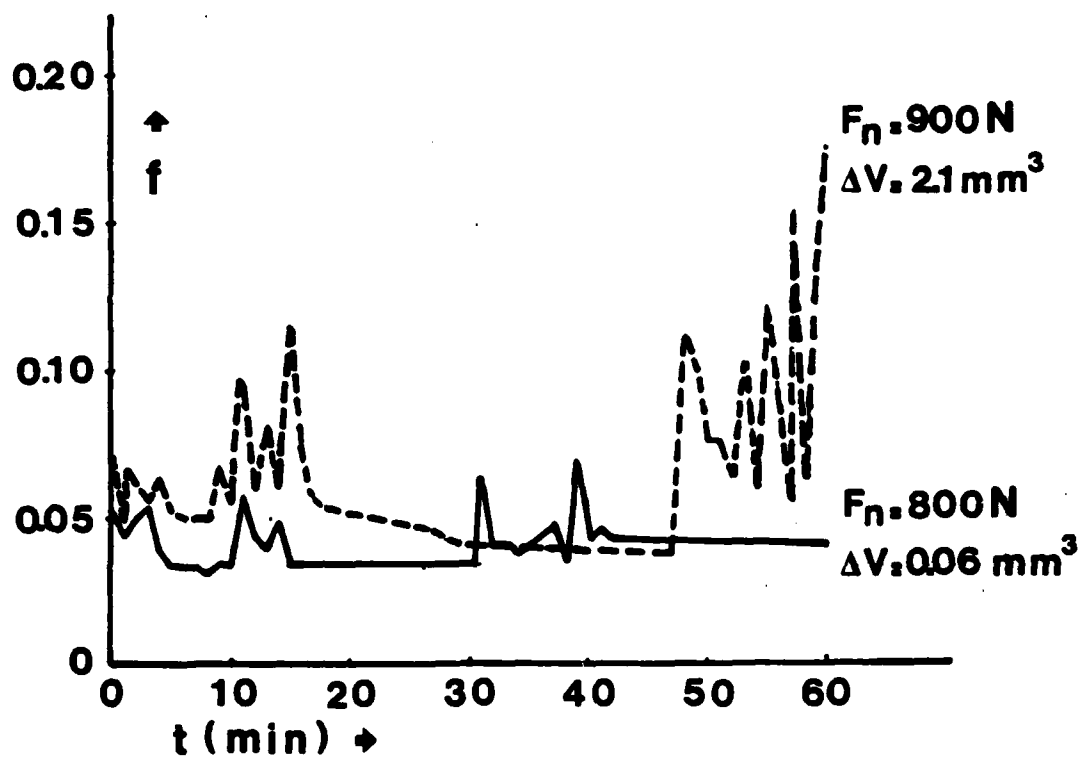


Fig. 3 Coefficient of friction versus time for two tests, performed with liquid-nitrided surfaces of steel 42CrMo4 (E).

F_N = normal force

ΔV = volume wear, measured after termination of the tests.

No running-in ($d^* = 0\text{ m}$).

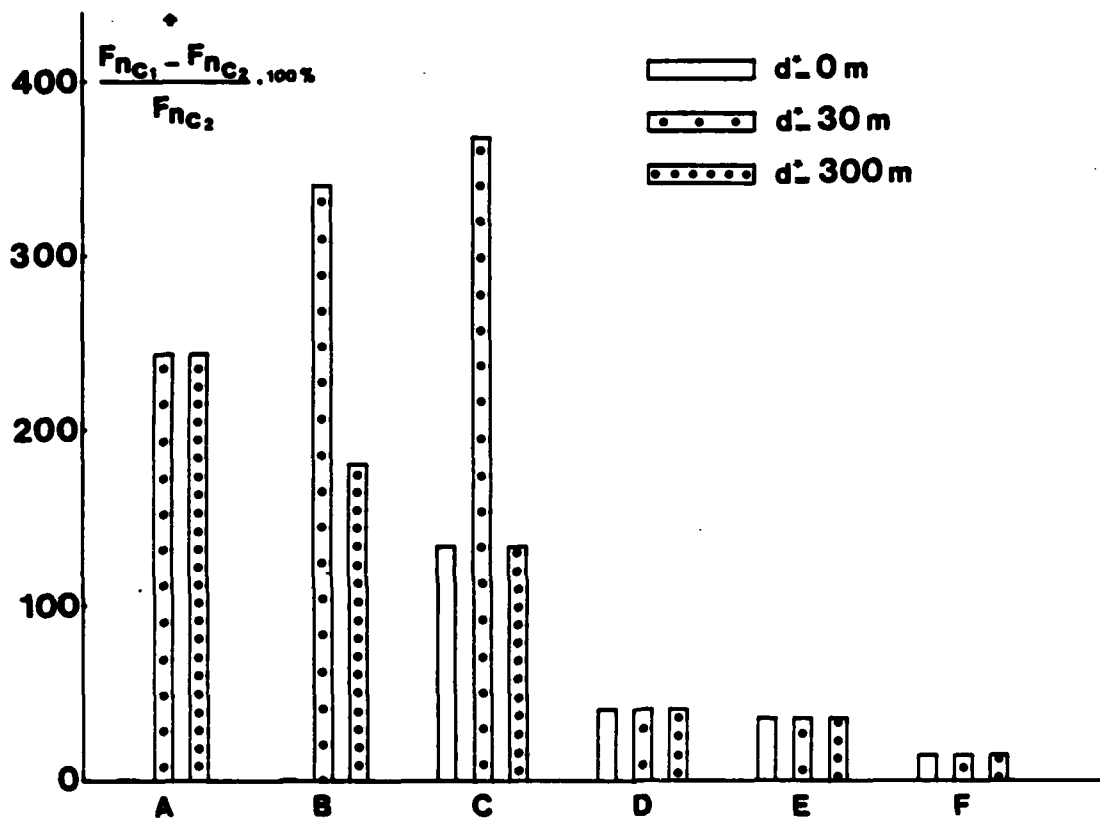


Fig. 4 The relative difference $\frac{F_{Nc1} - F_{Nc2}}{F_{Nc2}} \cdot 100\%$ for six different surfaces.

A-F : for explanation see Table 1
 d^* : running-in distance

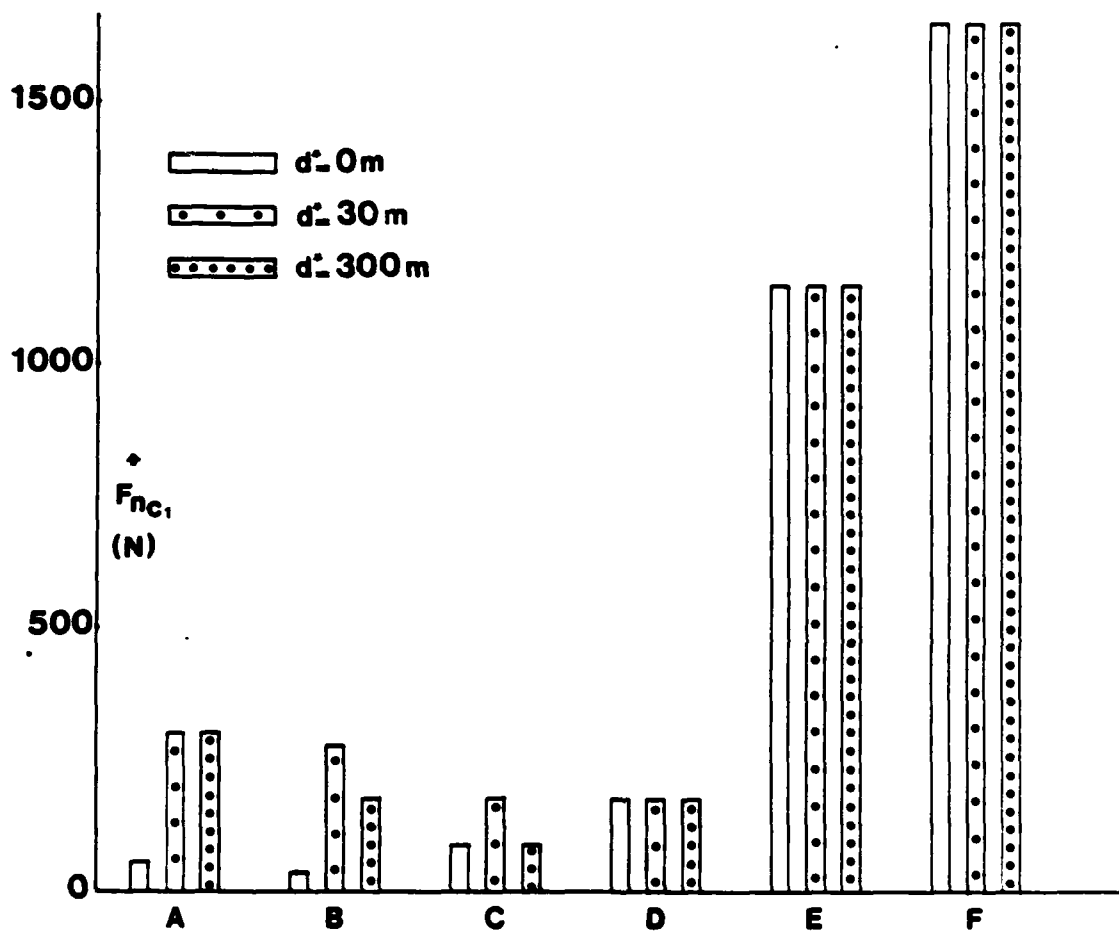


Fig. 5 Critical load value for immediate film collapse F_{NC2} for six different surfaces.

A-F : for explanation see Table 1
 d^* : running-in distance.

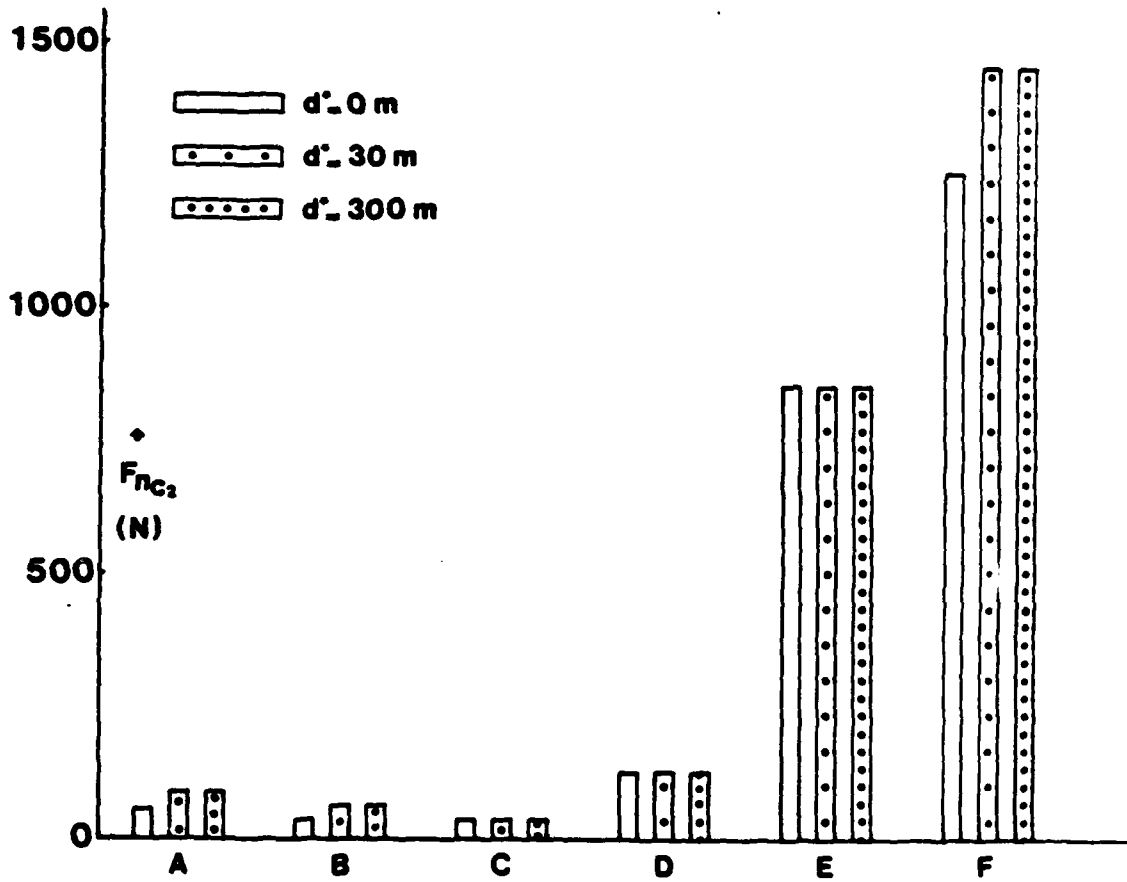
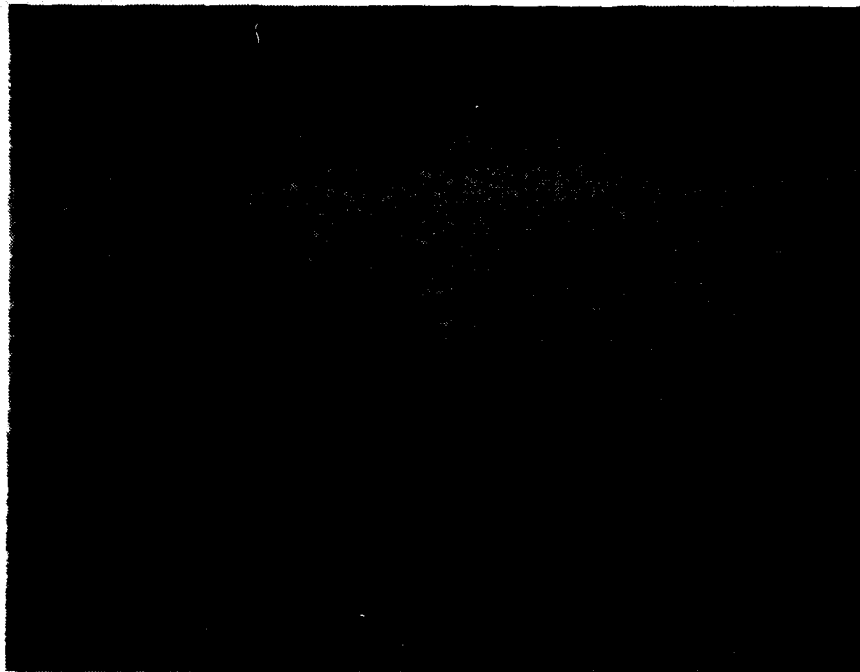


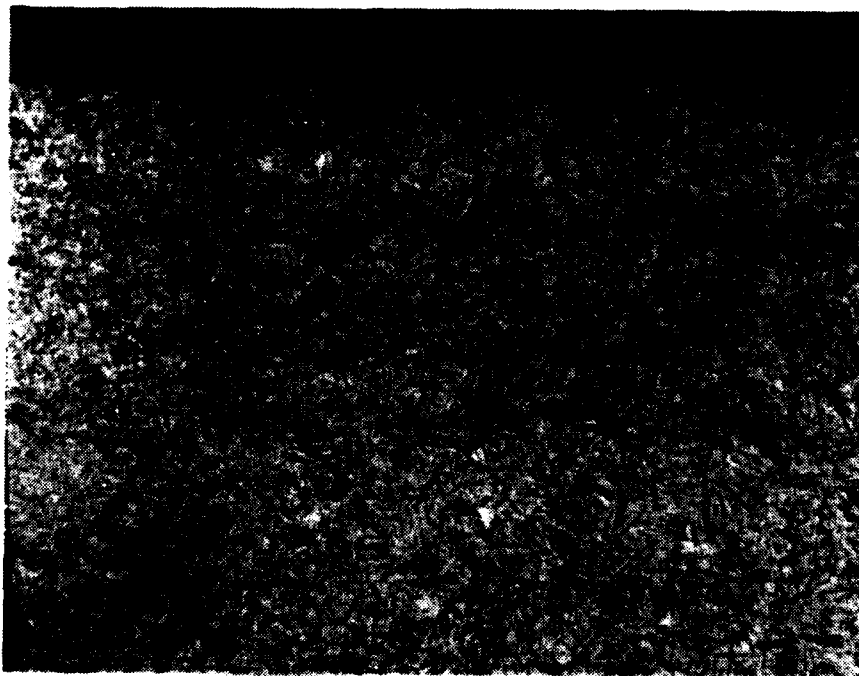
Fig. 6 Critical load for delayed film collapse F_{NC1} for six different surfaces.

A-F : for explanation see Table 1
 d^* : running-in distance.



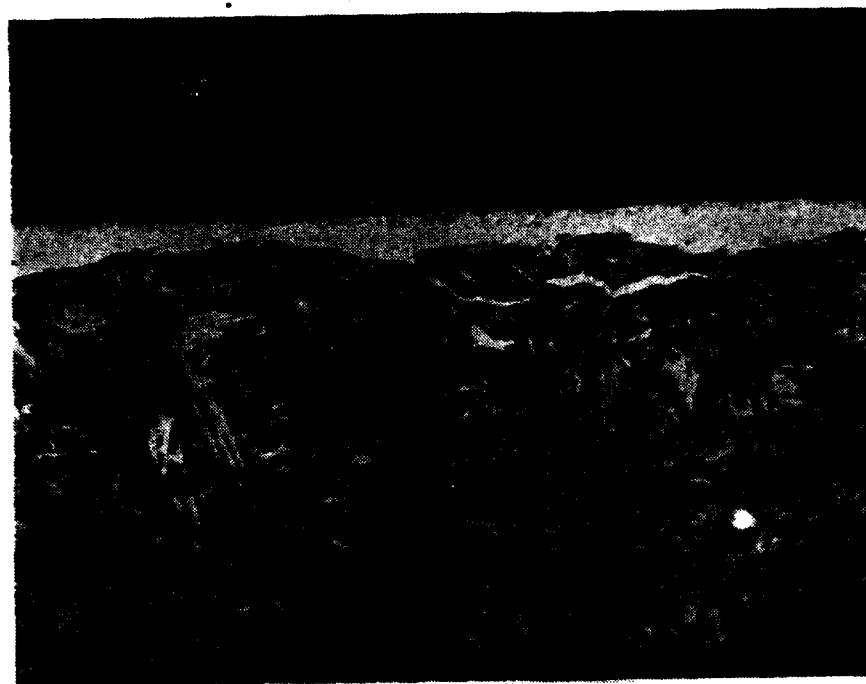
1mm

Fig. 7 Structure of surface zone of material B.



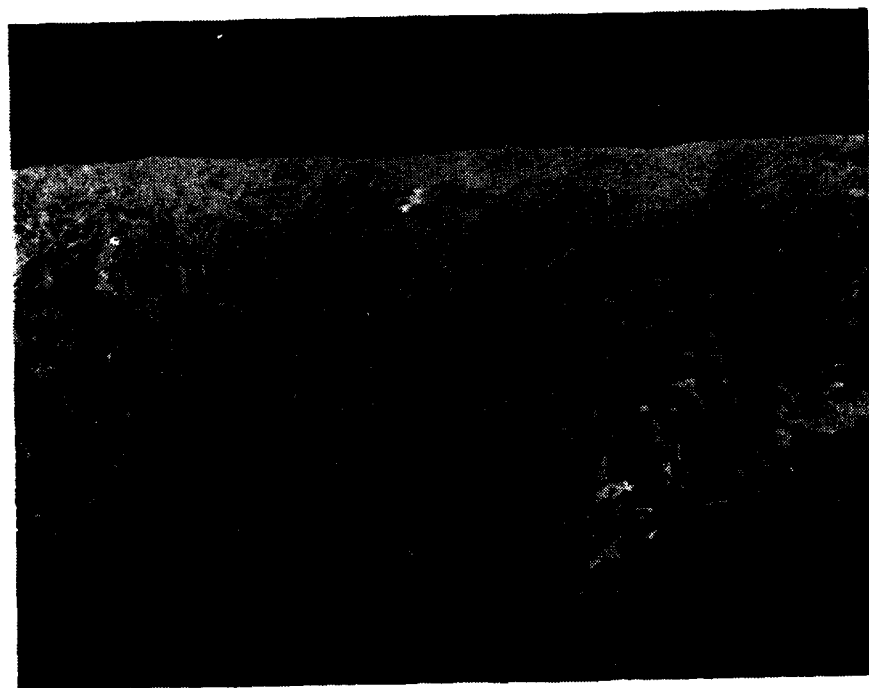
100 μm

Fig. 8 Structure of surface zone of material B.



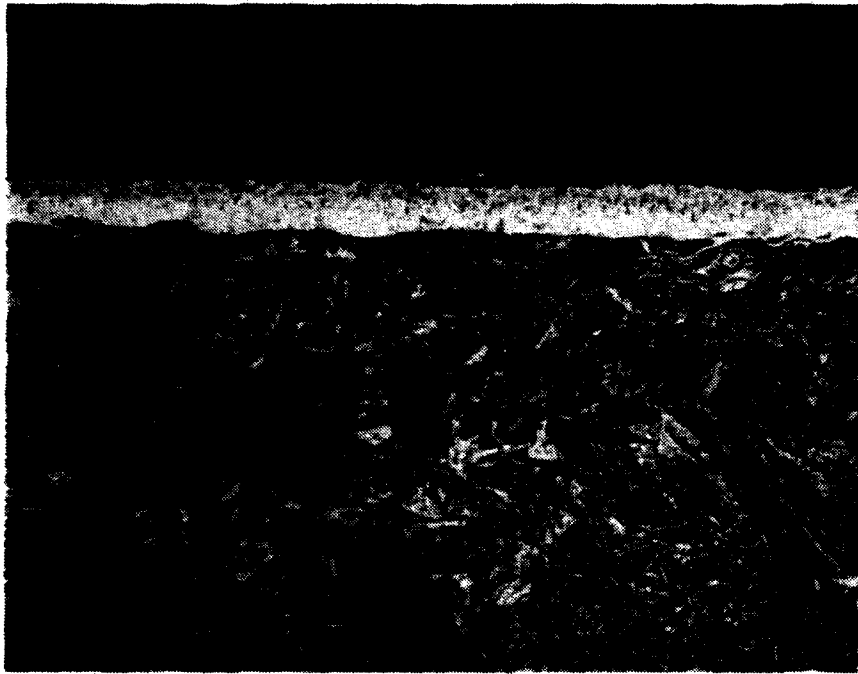
100 μm

Fig. 9 Structure of surface zone of material C.



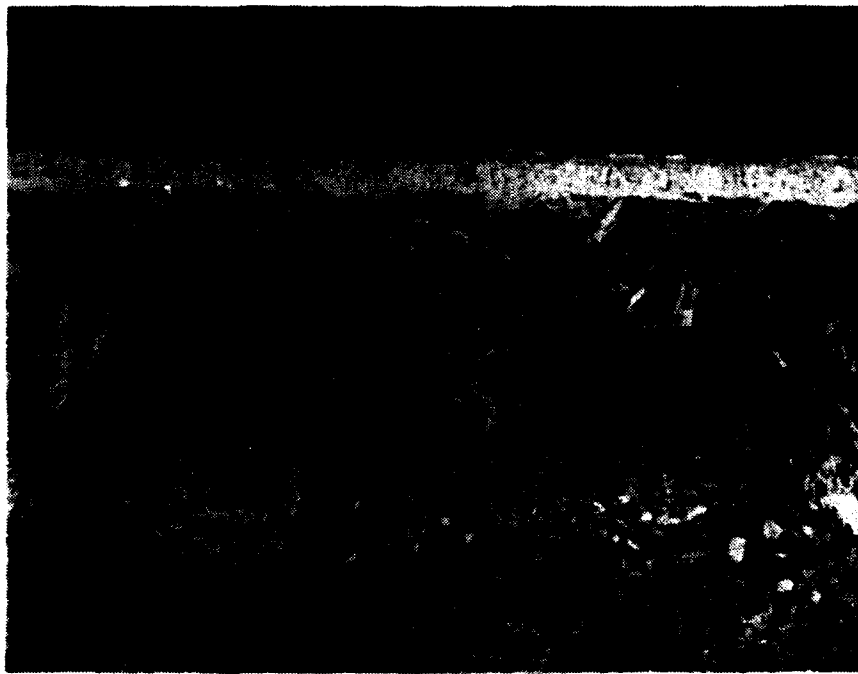
100 μm

Fig. 10 Structure of surface zone of material D.



100 μm

Fig. 11 Structure of surface zone of material E.



100 μm

Fig. 12 Structure of surface zone of material F.

END

Filmed

1-84

DTIC